Photoacoustics 27 (2022) 100389

Contents lists available at ScienceDirect

Photoacoustics

journal homepage: www.elsevier.com/locate/pacs

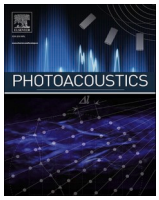

All-optical light-induced thermoacoustic spectroscopy for remote and non-contact gas sensing

Yufeng Pan [a,b,1], Jinbiao Zhao [a,b,1], Ping Lu [a,b,c,*], Chaotan Sima [a,b,c], Wanjin Zhang [a], Lujun Fu [a], Deming Liu [a,b], Jiangshan Zhang [d], Hongpeng Wu [e], Lei Dong [e,*]

[a] Wuhan National Laboratory for Optoelectronics (WNLO) and National Engineering Research Center of Next Generation Internet Access-system, School of Optical and Electronic Information, Huazhong University of Science and Technology, Wuhan 430074, China
[b] Shenzhen Huazhong University of Science and Technology Research Institute, Shenzhen 518000, China
[c] Wuhan OV Optical Networking Technology Co., Ltd., Wuhan 430074, China
[d] Department of Electronics and Information Engineering, Huazhong University of Science and Technology, Wuhan 430074, China
[e] State Key Laboratory of Quantum Optics and Quantum Optics Devices, Institute of Laser Spectroscopy and Collaborative Innovation Center of Extreme Optics, Shanxi University, Taiyuan 030006, China

ARTICLE INFO

Keywords:
Light-induced thermoacoustic spectroscopy
Gas sensor
Quartz tuning fork
Fiber-optic Fabry-Pérot interferometry technique
Hydrogen sulfide detection

ABSTRACT

All-optical light-induced thermoacoustic spectroscopy (AO-LITS) is reported for the first time for highly sensitive and selective gas sensing, in which a commercial standard quartz tuning fork (QTF) is employed as a photothermal detector. The vibration of the QTF was measured by the highly sensitive fiber-optic Fabry-Pérot (FP) interferometry (FPI) technique, instead of the piezoelectric detection in the conventional LITS. To improve the stability of the sensor system, a compact QTF-based fiber-optic FPI module is fabricated by 3D printing technique and a dual-wavelength demodulation method with the ellipse-fitting differential-cross-multiplication algorithm (DW-EF-DCM) is exploited for the FPI measurement. The all-optical detection scheme has the advantages of remote detection and immunity to electromagnetic interference. A minimum detection limit (MDL) of 422 ppb was achieved for hydrogen sulfide (H_2S), which was ~ 3 times lower than a conventional electrical LITS sensor system. The AO-LITS can provide a promising approach for remote and non-contact gas sensing in the whole infrared spectral region.

1. Introduction

Quart tuning fork (QTF) as a resonant acoustic-electric transducer based on its piezoelectric property has been successfully applied in trace gas photoacoustic sensing since 2002, which is called quartz-enhanced photoacoustic spectroscopy (QEPAS) [1–8]. The QTF has the advantages of a high resonance frequency, a high quality factor, a small size and a low cost, which enable the QEPAS sensor to have the immunity to ambient acoustic noise and the capability to analyze ultra-small volume gas samples with respect to the conventional PAS sensor based on a photoacoustic cell and a microphone [9–23]. However, the QTF required to be immersed in the target gas in the QEPAS sensor, so that the QTF can be corroded. Thus, the performance of the QTF can be deteriorated as detecting the corrosive gas for a long time, which limits the application of the QEPAS sensor in some harsh environments such as combustion field.

Light-induced thermoacoustic spectroscopy (LITS) as a laser-absorption-spectroscopy-based gas sensing approach was first reported in 2018 [24], which used a QTF as a photothermal detector. Different from measuring acoustic signal generated by gas absorption of light energy in a QEPAS sensor, the QTF is exploited to measure the absorption variation of light intensity in a LITS sensor, and the light beam is directed on the QTF's surface instead of between the gap of QTF's prongs. The thermal energy generated by light absorption is transformed into the mechanical vibration of the QTF by the light-thermo-elastic conversion, and subsequently the mechanical vibration is enhanced due to the resonant characteristic of the QTF [24–30]. The mechanical vibration of the QTF can also generate acoustic waves and be detected [31]. The LITS sensor system is similar to that of tunable diode laser absorption spectroscopy (TDLAS), except that the commercial

* Corresponding author.
E-mail addresses: pluriver@mail.hust.edu.cn (P. Lu), donglei@sxu.edu.cn (L. Dong).
[1] These authors contributed equally to this manuscript.

https://doi.org/10.1016/j.pacs.2022.100389
Received 9 June 2022; Received in revised form 9 August 2022; Accepted 9 August 2022
Available online 10 August 2022

photodetector is replaced by the QTF. Therefore, the LITS sensor can realize the non-contact measurement in contrast to the conventional PAS/QEPAS sensor. Compared with the conventional commercial photodetector-based TDLAS technique, the QTF-based LITS technique has the merits of low cost, small size, high sensitivity, large power dynamic range and signal enhancement by increasing of the excitation laser power, and in particular it can achieve the trace gas detection in the whole infrared spectral region, even THz spectral region, without requiring any cooling system [24–34]. However, the conventional piezoelectric measurement is vulnerable to electromagnetic interference and difficult to achieve long-distance remote detection.

For toxic and corrosive gas (e.g. H_2S) detection, the remote and non-contact measurement is expected. In some specific fields (e.g. power industry), the gas sensor also required to be immune to severe electromagnetic interference. In fact, fiber-optics sensing technique based on Fabry-Pérot interferometry (FPI) structure, can offer a safe and effective approach to remotely measure the vibration of the QTF not depending on its piezoelectric effect, thus effectively avoiding electromagnetic interference. For the FPI detection, there are several algorithms. The conventional quadrature working point (Q-point) demodulation method can be affected by the instability of Q-point and the dynamic range is limited by the linear region of interference spectrum [35–38]. The white-light-based phase demodulation method cannot demodulate the high-frequency signal (such as ~ 32 kHz for the QTF) [14,39,40]. Therefore, the dual-wavelength demodulation method with the ellipse-fitting differential-cross-multiplication algorithm (DW-EF-DCM) is exploited to measure the vibration of the QTF in this work, which has the advantages of good stability, strong robustness, large demodulation frequency range and large dynamic range, and which is not affected by the instability of Q-point [41–43].

In this paper, we develop an all-optical LITS (AO-LITS) sensor to detect H_2S for the first time. The LITS technique is used to provide the capability of non-contact measurement. The vibration of the QTF produced by the light-induced thermo-elastic effect is measured by the fiber-optic FPI technique instead of the conventional piezoelectric detection. A 1576.29 nm distributed feedback (DFB) laser is used as an excitation light source for the H_2S detection. A Herriot multipass gas cell (MGC) with an effective optical pathlength of 3.3 m is used to enhance the light absorption of the H_2S gas. To improve the stability and practicability of the sensor system, a QTF-based integrated fiber-optic FPI module is designed and fabricated by means of the 3D printing technique. The DW-EF-DCM demodulation method was innovatively applied in the developed AO-LITS sensor system. The fiber-optic interferometry technique makes the sensor system have the abilities of remote detection and immunity to electromagnetic interference. Such an AO-LITS sensor system can also be suitable for trace gas remote detection in the mid-infrared, far-infrared and even THz spectral regions since the quartz crystal has an inherent light absorption in a broad spectral region and the probe laser of the fiber-optic FPI technique is independent of the excitation light for gas absorption.

2. Theory and design of AO-LITS sensor

2.1. QTF-based fiber-optic FPI module

In a QTF-based AO-LITS sensor, the information of target gas concentration can be obtained by measuring the vibration of the QTF. A commercial standard QTF and the fiber-optic FPI probe were integrated to a compact module using 3D printing technique. Fig. 1(a) and (b) show the 3D schematic diagram and physical photograph of the module, respectively. The module with dimensions of 20 mm × 14 mm × 14 mm consisted of two same interchangeable windows, a commercial standard QTF, a ceramic ferrule, a ceramic sleeve and an optical fiber. The two same interchangeable windows with a diameter of 12.7 mm were installed on the front and back of the QTF, respectively, which was employed to insulate the external environment and allow access to the laser beam. The resonance frequency and the quality factor of the used QTF at atmospheric pressure were experimentally determined to be 32,776.2 Hz and 10,283.5, respectively. The ceramic ferrule was employed to fix the optical fiber. The end surface of the optical fiber and the silver-coated surface of the QTF's prong formed a low-finesse F-P cavity. The ceramic sleeve was used to assist in fixing the ceramic ferrule. All these parts were fixed and sealed by Torr Seal Epoxy.

2.2. DW-EF-DCM demodulation method based on QTF vibration

Fig. 2 shows the schematic diagram of a FPI detection unit for QTF vibration measurement based on dual-wavelength demodulation technique. A near-infrared tunable laser source (Alnair Labs, TLG-210) was employed as the probe light source to generate two probe laser beams with the different wavelengths around 1550 nm. Multiplexing and demultiplexing of the two probe laser beams were achieved by means of

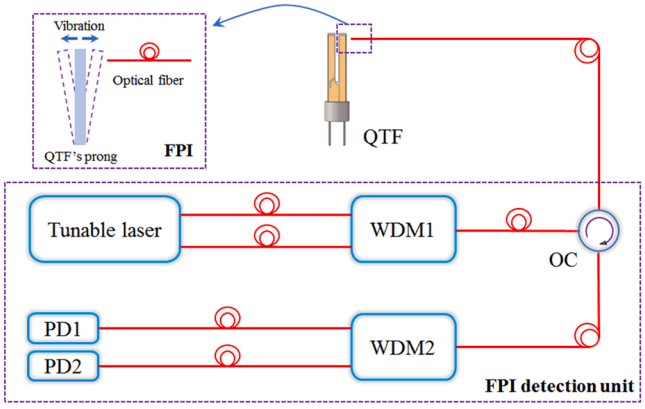

Fig. 2. FPI detection unit for QTF vibration measurement based on dual-wavelength demodulation technique: WDM, wavelength division multiplexer; OC, optical circulator; PD, photodetector.

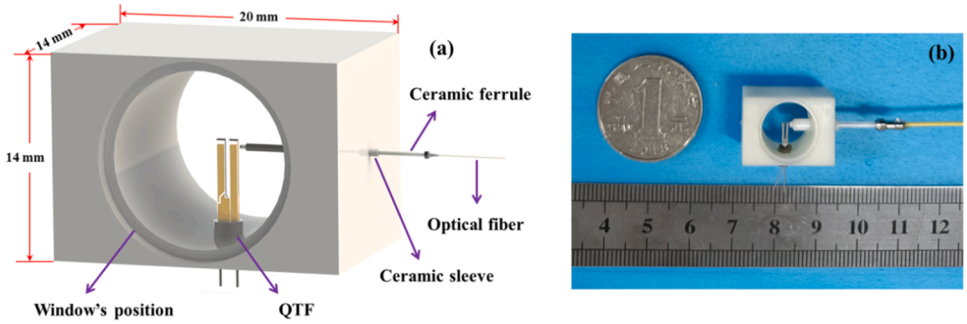

Fig. 1. (a) 3D schematic diagram of the QTF-based fiber-optic FPI module (b) Physical photograph of the FPI module.

two wavelength division multiplexers. A fiber-coupled optical circulator was used to separate incident light and reflected light for the QTF-based F-P cavity. The interferometric signals of the two probe laser beams were detected by two commercial fiber-coupled photodetectors (PDs), respectively. All the components of the dual-wavelength demodulation system were connected using the optical fibers. The output signals of the two PDs were recorded by a data acquisition (DAQ) card (National Instrument, PCIe-6376).

In the QTF-based F-P cavity, the vibration of the QTF's prong causes the F-P cavity length to oscillate. The signal obtained by each PD can be described as [41–43]:

$$V_1 = A_1 + B_1 cos[\frac{4\pi nL}{\lambda_1} + \varphi(t)] \quad (1)$$

$$V_2 = A_2 + B_2 cos[\frac{4\pi nL}{\lambda_2} + \varphi(t)] \quad (2)$$

where V_1 and V_2 represent the output signals of PD1 and PD2, respectively. A_1, A_2, B_1 and B_2 are constant coefficients determined by the probe laser and the PDs, L is the F-P cavity length, n is the refractive index of air in the F-P cavity, λ_1 and λ_2 are the two probe laser wavelengths, respectively, $\varphi(t)$ is the phase signal of the QTF vibration, t is time. The phase difference of the two probe laser wavelengths can be expressed as:

$$\Delta\varphi = \frac{4\pi nL}{\lambda_1} - \frac{4\pi nL}{\lambda_2} \quad (3)$$

when $\Delta\varphi \neq k\pi$ (k is a integer), there is an elliptical relationship between V_1 and V_2. The A_1, A_2, B_1, B_2 and $\Delta\varphi$ can be obtained by ellipse fitting. The output signals of the two PDs can be normalized by eliminating direct current component and alternating current amplitude. The normalized signals of V_1 and V_2 can be expressed as:

$$V_{1n} = (V_1 - A_1)/B_1 = cos[\frac{4\pi nL}{\lambda_1} + \varphi(t)] \quad (4)$$

$$V_{2n} = (V_2 - A_2)/B_2 = cos[\frac{4\pi nL}{\lambda_2} + \varphi(t)] \quad (5)$$

The phase signal of the QTF vibration can be calculated by using DCM algorithm:

$$\varphi(t) = \frac{\int (V'_{1n} V_{2n} - V_{1n} V'_{2n}) dt}{sin(\Delta\varphi)} \quad (6)$$

where V'_{1n} and V'_{2n} are the derivatives of V_1 and V_2, respectively. The vibration amplitude of the QTF related to the oscillation amplitude of the F-P cavity length, can be obtained by demodulating $\varphi(t)$ at 32,776.2 Hz (the resonance frequency of the used QTF) using a lock-in amplifier.

To obtain the fitted ellipse of the QTF-based F-P cavity, the FPI module and detection unit ran for one hour. Affected by the environmental parameters such as temperature and humidity, the refractive index of air in the cavity drifted, resulting in the changes of the signals of the two PDs, which is plotted in Fig. 3(a) and (b), respectively. With the PD1 and PD2 signals as the abscissa and ordinate, respectively, an ellipse was achieved as shown in Fig. 3(c). After an ellipse fitting, A_1, B_1, A_2, B_2 and $\Delta\varphi$ were achieved to be 1.0493, 1.0008, 0.9751, 0.9342 and 0.4530π, respectively.

3. Experimental results and discussions

3.1. Experiment setup and optimization

H_2S as a toxic and corrosive gas was chosen as the analyte due to the widely detection demand in environmental monitoring, chemical production and power industry [44–50]. Fig. 4 shows the experimental setup of the AO-LITS sensor system for H_2S detection. A continuous wave DFB fiber-coupled diode laser with an output power of ~ 20 mW

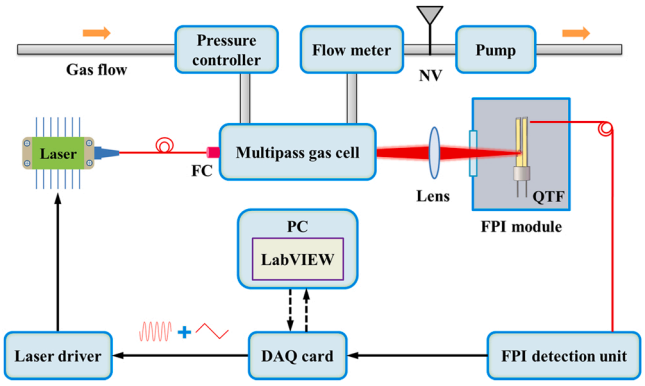

Fig. 4. Experiment setup of the AO-LITS sensor system: FC, fiber-coupled collimator; NV, needle valve; PC, personal computer.

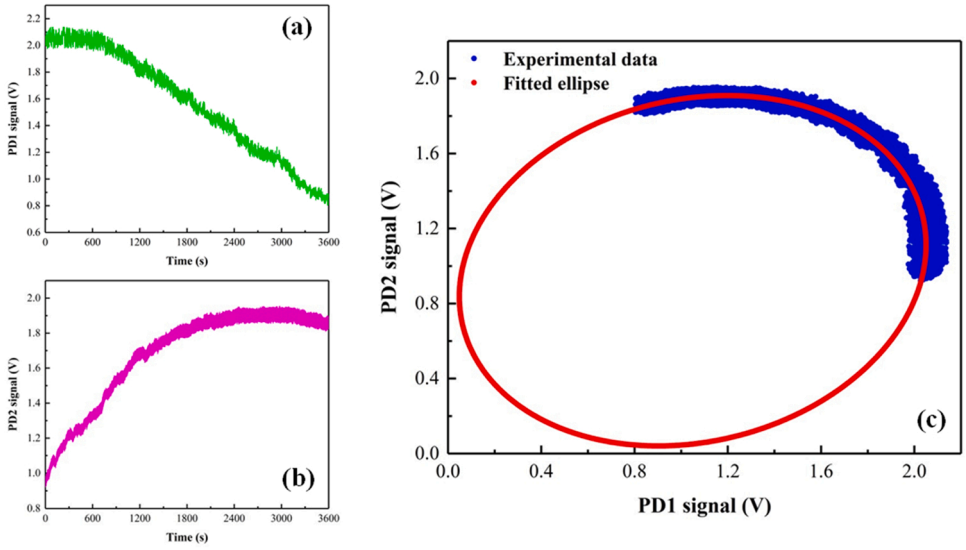

Fig. 3. (a) Output signals of PD1 (b) Output signals of PD2 (c) Ellipse fitting for the combined signals of PD1 and PD2.

was selected as an excitation light source to detect H_2S at 1576.29 nm, where has an interference-free H_2S absorption line [51]. The laser operating temperature and current were controlled by an integrated laser driver (Wavelength Electronics, LDTC0520). Wavelength modulation spectroscopy (WMS) and second-harmonic (2 *f*) detection technique were exploited to improve the signal-to-noise ratio (SNR). A triangular signal plus a sinusoidal signal of 16,388.1 Hz (half of the resonance frequency of the used QTF) were generated by a LabVIEW controlled DAQ card to scan and modulate the laser current, respectively, for 2 *f* signal detection. The output laser was collimated by a fiber-coupled collimator, and then injected into a compact Herriot MGC (Healthy Photon, HPHC-B). The MGC has an effective optical pathlength of 3.3 m with 33 optical passes to enhance light absorption of H_2S gas. The output laser emitted from the MGC was focused to the bottom of the QTF's prongs by a flat-convex focusing lens with a 30 mm focal length, which is the optimum laser focal point for LITS proved in Ref. [25]. The positions of the MGC and the QTF-based FPI module were adjusted using a high precision three-axis translation stage. The pressure in the QTF-based FPI module was atmospheric pressure, which avoided the use of any pressure control unit. A LabVIEW-based lock-in amplifier (LIA) demodulated the phase signals from the FPI detection unit in 2-*f* mode at 32,776.2 Hz. The time constant and the filter slope of the LIA were set to 300 ms and 12 dB/oct, respectively, corresponding to an equivalent noise bandwidth (ENBW) of 0.416 Hz. All data were recorded and processed by a LabVIEW software program in a personal computer.

Since H_2S is toxic, the MGC uses a closed structure with a gas inlet and outlet. The pressure in the MGC was maintained at atmospheric pressure by a mini diaphragm pump (KNF Technology, N813.5ANE) and a pressure controller (MKS Instruments, 649B13TS1M22M). A needle valve and a mass flow meter (Alicat Scientific, M-2SLPM-D/5M) were used to control the gas flow rate at 150 mL/min. A 50 ppm H_2S/N_2 standard gas was diluted with pure N_2 to produce H_2S/N_2 mixtures with different H_2S concentration levels using a gas dilution system (MCQ Instruments, GB100). For field applications, the MGC can be open. In this case, no gas control unit is required. In addition, the AO-LITS can also be applied in an open environment (without the gas cell).

To improve the AO-LITS signal amplitude, the laser wavelength modulation depth was optimized. The MGC was filled with 50 ppm H_2S/N_2 gas mixture and operated at atmospheric pressure. The laser wavelength was tuned to the peak of the target H_2S absorption line. The 16,388.1 Hz sinusoidal signal was used to modulate the laser driving current with the modulation depth from 4 mA to 18 mA. Fig. 5 shows the measured AO-LITS signal amplitudes under different modulation depths. According to the results, the modulation depth was set at 12 mA to obtain the strongest AO-LITS signal amplitude in the following investigations.

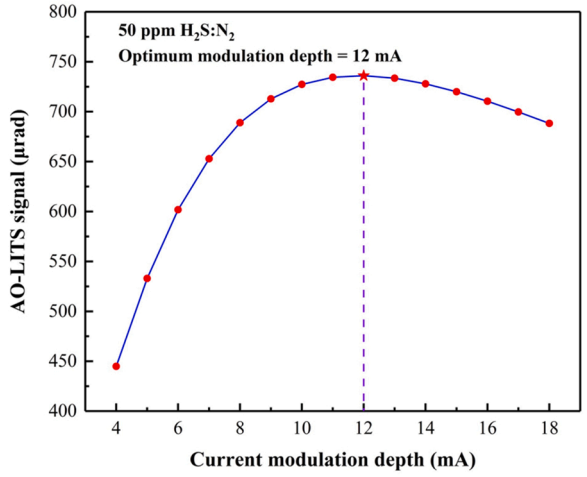

Fig. 5. Signal amplitude as a function of current modulation depth.

3.2. Performance evaluation of the AO-LITS sensor system

The measured 2 *f* spectrum of 50 ppm H_2S (solid line) at atmospheric pressure was shown in Fig. 6(a). The noise level of the AO-LITS sensor system was evaluated. Pure N_2 was flushed into the MGC. The measured noise was depicted in Fig. 6(b). As a comparison, a conventional electrical LITS (E-LITS) scheme [25] was implemented with the same experimental conditions. The measured 2 *f* spectrum of 50 ppm H_2S and noise of pure N_2 by piezoelectric detection were plotted in Fig. 6(a) (dash line) and Fig. 6(c), respectively. It can be found that the SNR of AO-LITS is ~ 3 times stronger than that of E-LITS.

The linearity of the concentration response of the sensor system was evaluated by five different H_2S concentration levels ranging from 10 ppm to 50 ppm. The laser wavelength was tuned to the peak of the target H_2S absorption line to obtain the 2 *f* signal amplitude. Sixty data points of the 2 *f* signal amplitudes were recorded continuously with a 1 s data acquisition time at each H_2S concentration level, as shown in Fig. 7 (a). The average values of the measured results for each step as a function of the H_2S concentrations were plotted in Fig. 7(b). It confirms the linear response of the AO-LITS sensor system to H_2S concentrations by a linear fitting with a R-square value of > 0.999. Based on the slope of the fitting curve and 1σ noise of pure N_2, a H_2S minimum detection limit (MDL) of 422 ppb was achieved (MDL = 1σ noise/slope) [52]. The noise equivalent absorption (NEA) coefficient and the normalized noise equivalent absorption (NNEA) coefficient can be calculated by the following equations [4,25]:

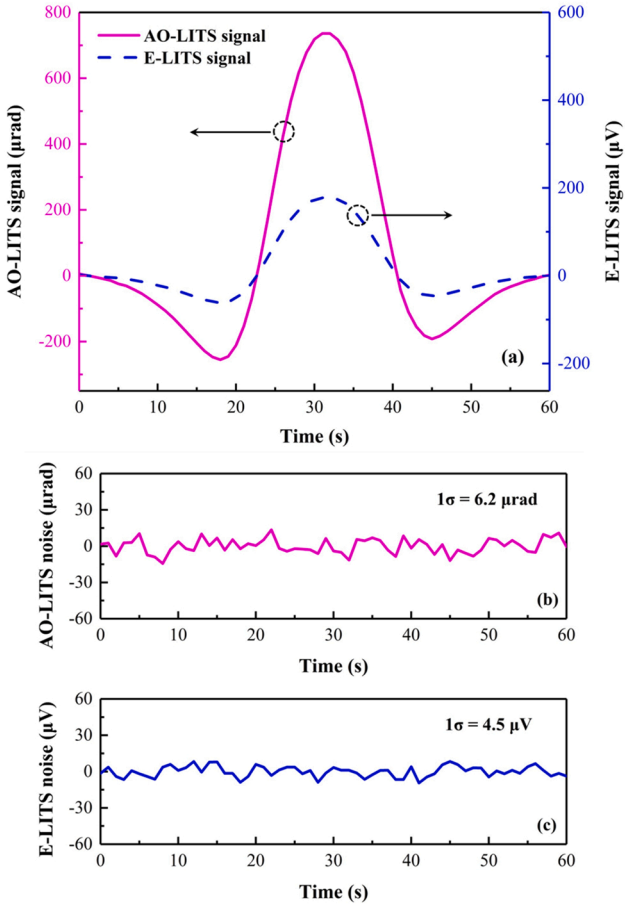

Fig. 6. (a) 2 *f* spectrum measured by AO-LITS (solid line) and E-LITS (dash line) (b) AO-LITS noise level (c) E-LITS noise level.

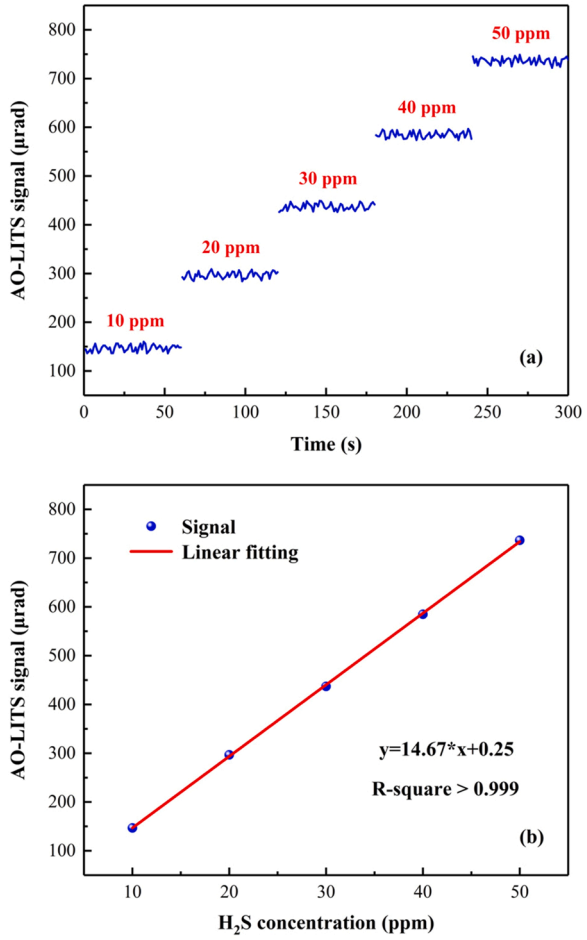

Fig. 7. (a) AO-LITS signals at the different H_2S concentration levels (b) Response linearity of the AO-LITS sensor system.

$$\mathrm{NEA} = \frac{\alpha_{min}}{\sqrt{\mathrm{ENBW}}} \tag{7}$$

$$\mathrm{NNEA} = \mathrm{P} \bullet \mathrm{NEA} \tag{8}$$

α_{min} is the minimum detectable absorption coefficient, which can be calculated to be 1.5×10^{-8} cm^{-1} by the HITRAN database [51]. ENBW is the equivalent noise bandwidth of the LIA, which is 0.416 Hz, when the time constant and the filter slope of the LIA were set to 300 ms and 12 dB/oct, respectively. P is the excitation laser power of ~ 20 mW. Hence, the NEA coefficient and the NNEA coefficient were determined to be 2.3×10^{-8} $\mathrm{cm}^{-1}/\sqrt{\mathrm{Hz}}$ and 4.6×10^{-10} $\mathrm{W \cdot cm}^{-1}/\sqrt{\mathrm{Hz}}$, respectively.

3.3. *Long-time stability of the AO-LITS sensor system*

To verify the long-time stability of the developed AO-LITS sensor system, the 50 ppm H_2S was continuously measured for one hour. The laser wavelength was tuned to the peak of the target H_2S absorption line. The measurement results are shown in the Fig. 8 (red line). Since the dual-wavelength demodulation system can degrade into the conventional Q-point demodulation system when only one wavelength is used, we measured the 50 ppm H_2S using the conventional Q-point demodulation method, as shown in Fig. 8 (blue line). It can be observed that when the operating time exceeded ~ 1000 s, the signal began to drop, which meant that the working point drifted (not at Q-point). However, the signals remained stable for the DW-EF-DCM demodulation method. The experimental results confirmed that the developed AO-LITS gas sensor based on the DW-EF-DCM demodulation method has a good stability for long-time gas detection.

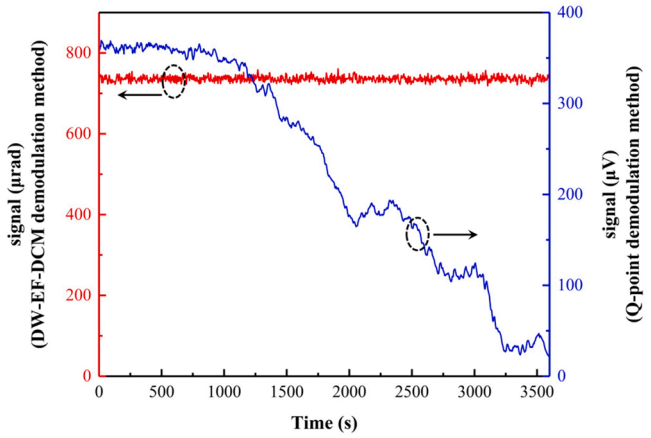

Fig. 8. Comparison of DW-EF-DCM demodulation method (red line) and Q-point demodulation method (blue line) for the AO-LITS sensor system.

4. Conclusions

In this work, a novel AO-LITS gas sensor system based on fiber-optic FPI measurement was reported by using the DW-EF-DCM demodulation method. A compact QTF-based fiber-optic FPI module was designed and the vibration of the QTF was measured by the FPI technique. At atmospheric pressure, the MDL for H_2S detection is 422 ppb, which is ~ 3 times better than that of the conventional electrical LITS sensor system. Since the QTF does not need to be in contact with the target gas, the AO-LITS can realize non-contact measurement and avoid the interference of gas flow noise on highly-sensitive optical detection [13,14]. The detection sensitivity can be further improved by decreasing the operating pressure in the QTF-based FPI module (to obtain a higher quality factor of the QTF) and/or increasing the effective optical pathlength [25, 53]. With respect to E-LITS, AO-LITS removes the restriction on the use of piezoelectric materials. In addition, the DW-EF-DCM demodulation method has large dynamic range for vibration measurement. As a result, with the same geometry of tuning fork, the materials with a higher laser absorption coefficient (such as black phosphorus and perovskite) and with a lower Young's modulus (such as KBr and KCl) could offer higher sensitivity [54–56]. On the other hand, since the DW-EF-DCM algorithm can be affected by the instability of the probe laser power in the case of continuous operation for a very long time (such as several days), the optimization of the demodulation algorithm for FPI measurement will also be our next research work, in order to further improve the stability and calibration-free ability of the AO-LITS sensor system.

Declaration of Competing Interest

The authors declare that they have no known competing financial interests or personal relationships that could have appeared to influence the work reported in this paper.

Data Availability

Data will be made available on request.

Acknowledgement

The project is sponsored by National Key R&D Program of China (No. 2019YFE0118200); National Natural Science Foundation of China (62122045, 62175137, 62075119); NSFC-RS Exchange Programme (62111530153); Science, Technology and Innovation Commission of Shenzhen Municipality (2021Szvup089); Science Fund for Creative Research Groups of the Nature Science Foundation of Hubei (2021CFA033); The Shanxi Science Fund for Distinguished Young

Scholars (20210302121003); The Fundamental Research Funds for the Central Universities (HUST: YCJJ202201004).

References

[1] A.A. Kosterev, Y.A. Bakhirkin, R.F. Curl, F.K. Tittel, Quartz-enhanced photoacoustic spectroscopy, Opt. Lett. 27 (21) (2002) 1902–1904.

[2] A.A. Kosterev, F.K. Tittel, D.V. Serebryakov, A.L. Malinovsky, I.V. Morozov, Applications of quartz tuning forks in spectroscopic gas sensing, Rev. Sci. Instrum. 76 (4) (2005), 043105.

[3] N. Petra, J. Zweck, A.A. Kosterev, S.E. Minkoff, D. Thomazy, Theoretical analysis of a quartz-enhanced photoacoustic spectroscopy sensor, Appl. Phys. B 94 (2009) 673–680.

[4] H. Wu, L. Dong, H. Zheng, Y. Yu, W. Ma, L. Zhang, W. Yin, L. Xiao, S. Jia, F. K. Tittel, Beat frequency quartz-enhanced photoacoustic spectroscopy for fast and calibration-free continuous trace-gas monitoring, Nat. Commun. 8 (2017) 15331.

[5] P. Patimisco, A. Sampaolo, L. Dong, F.K. Tittel, V. Spagnolo, Recent advances in quartz enhanced photoacoustic sensing, Appl. Phys. Rev. 5 (1) (2018), 011106.

[6] A. Sampaolo, P. Patimisco, M. Giglio, A. Zifarelli, H. Wu, L. Dong, V. Spagnolo, Quartz-enhanced photoacoustic spectroscopy for multi-gas detection: A review, Anal. Chim. Acta 1202 (2022), 338894.

[7] H. Lin, H. Zheng, B.A.Z. Montano, H. Wu, M. Giglio, A. Sampaolo, P. Patimisco, W. Zhu, Y. Zhong, L. Dong, R. Kan, J. Yu, V. Spagnolo, Ppb-level gas detection using on-beam quartz-enhanced photoacoustic spectroscopy based on a 28 kHz tuning fork, Photoacoustics 25 (2022), 100321.

[8] F. Sgobba, A. Sampaolo, P. Patimisco, M. Giglio, G. Menduni, A.C. Ranieri, C. Hoelzl, H. Rossmadl, C. Brehm, V. Mackowiak, D. Assante, E. Ranieri, V. Spagnolo, Compact and portable quartz-enhanced photoacoustic spectroscopy sensor for carbon monoxide environmental monitoring in urban areas, Photoacoustics 25 (2022), 100318.

[9] A. Fathy, Y.M. Sabry, I.W. Hunter, D. Khalil, T. Bourouina, Direct absorption and photoacoustic spectroscopy for gas sensing and analysis: A critical review, Laser Photonics Rev. 16 (2022), 2100556.

[10] A. Miklós, P. Hess, Z. Bozóki, Application of acoustic resonators in photoacoustic trace gas analysis and metrology, Rev. Sci. Instrum. 72 (2001) 1937–1955.

[11] M.E. Webber, M. Pushkarsky, C.K.N. Patel, Fiber-amplifier-enhanced photoacoustic spectroscopy with near-infrared tunable diode lasers, Appl. Opt. 42 (12) (2003) 2119–2126.

[12] Y. Pan, L. Dong, X. Yin, H. Wu, Compact and highly sensitive NO_2 photoacoustic sensor for environmental monitoring, Molecules 25 (2020) 1201.

[13] H. Xiao, J. Zhao, C. Sima, P. Lu, Y. Long, Y. Ai, W. Zhang, Y. Pan, J. Zhang, D. Liu, Ultra-sensitive ppb-level methane detection based on NIR all-optical photoacoustic spectroscopy by using differential fiber-optic microphones with gold-chromium composite nanomembrane, Photoacoustics 26 (2022), 100353.

[14] K. Chen, H. Deng, M. Guo, C. Luo, S. Liu, B. Zhang, F. Ma, F. Zhu, Z. Gong, W. Peng, Q. Yu, Tube-cantilever double resonance enhanced fiber-optic photoacoustic spectrometer, Opt. Laser Technol. 123 (2020), 105894.

[15] L. Fu, P. Lu, C. Sima, J. Zhao, Y. Pan, T. Li, X. Zhang, D. Liu, Small-volume highly-sensitive all-optical gas sensor using non-resonant photoacoustic spectroscopy with dual silicon cantilever optical microphones, Photoacoustics 27 (2022), 100382.

[16] Y. Pan, L. Dong, H. Wu, W. Ma, L. Zhang, W. Yin, L. Xiao, S. Jia, F.K. Tittel, Cavity-enhanced photoacoustic sensor based on a whispering-gallery-mode diode laser, Atmos. Meas. Tech. 12 (2019) 1905–1911.

[17] Y. Liu, H. Lin, B.A.Z. Montano, W. Zhu, Y. Zhong, R. Kan, B. Yuan, J. Yu, M. Shao, H. Zheng, Integrated near-infrared QEPAS sensor based on a 28 kHz quartz tuning fork for online monitoring of CO_2 in the greenhouse, Photoacoustics 25 (2022), 100332.

[18] H. Zheng, Y. Liu, H. Lin, B. Liu, X. Gu, D. Li, B. Huang, Y. Wu, L. Dong, W. Zhu, J. Tang, H. Guan, H. Lu, Y. Zhong, J. Fang, Y. Luo, J. Zhang, J. Yu, Z. Chen, F. K. Tittel, Quartz-enhanced photoacoustic spectroscopy employing pilot line manufactured custom tuning forks, Photoacoustics 17 (2020), 100158.

[19] G. Aoust, R. Levy, M. Raybaut, A. Godard, J.M. Melkonian, M. Lefebvre, Theoretical analysis of a resonant quartz-enhanced photoacoustic spectroscopy sensor, Appl. Phys. B 123 (2017) 63.

[20] H. Lv, H. Zheng, Y. Liu, Z. Yang, Q. Wu, H. Lin, B.A.Z. Montano, W. Zhu, J. Yu, R. Kan, Z. Chen, F.K. Tittel, Radial-cavity quartz-enhanced photoacoustic spectroscopy, Opt. Lett. 46 (16) (2021) 3917–3920.

[21] H. Zheng, L. Dong, H. Wu, X. Yin, L. Xiao, S. Jia, R.F. Curl, F.K. Tittel, Application of acoustic micro-resonators in quartz-enhanced photoacoustic spectroscopy for trace gas analysis, Chem. Phys. Lett. 691 (2018) 462–472.

[22] S. Li, J. Lu, Z. Shang, X. Zeng, Y. Yuan, H. Wu, Y. Pan, A. Sampaolo, P. Patimisco, V. Spagnolo, L. Dong, Compact quartz-enhanced photoacoustic sensor for ppb-level ambient NO_2 detection by use of a high-power laser diode and a grooved tuning fork, Photoacoustics 25 (2022), 100325.

[23] X. Yin, L. Dong, H. Wu, M. Gao, L. Zhang, X. Zhang, L. Liu, X. Shao, F.K. Tittel, Compact QEPAS humidity sensor in SF_6 buffer gas for high-voltage gas power systems, Photoacoustics 25 (2022), 100319.

[24] Y. Ma, Y. He, Y. Tong, X. Yu, F.K. Tittel, Quartz-tuning-fork enhanced photothermal spectroscopy for ultra-high sensitive trace gas detection, Opt. Express 26 (24) (2018) 32103–32110.

[25] Y. He, Y. Ma, Y. Tong, X. Yu, F.K. Tittel, Ultra-high sensitive light-induced thermoelastic spectroscopy sensor with a high Q-factor quartz tuning fork and a multipass cell, Opt. Lett. 44 (8) (2019) 1904–1907.

[26] S.D. Russo, A. Zifarelli, P. Patimisco, A. Sampaolo, T. Wei, H. Wu, L. Dong, V. Spagnolo, Light-induced thermo-elastic effect in quartz tuning forks exploited as a photodetector in gas absorption spectroscopy, Opt. Express 28 (13) (2020) 19074–19084.

[27] L. Hu, C. Zheng, Y. Zhang, J. Zheng, Y. Wang, F.K. Tittel, Compact all-fiber light-induced thermoelastic spectroscopy for gas sensing, Opt. Lett. 45 (7) (2020) 1894–1897.

[28] Y. Ma, Recent advances in QEPAS and QEPTS based trace gas sensing: A review, Front. Phys. 8 (2020) 268.

[29] T. Wei, A. Zifarelli, S.D. Russo, H. Wu, G. Menduni, P. Patimisco, A. Sampaolo, V. Spagnolo, L. Dong, High and flat spectral responsivity of quartz tuning fork used as infrared photodetector in tunable diode laser spectroscopy, Appl. Phys. Rev. 8 (2021), 041409.

[30] S. Zhou, L. Xu, K. Chen, L. Zhang, B. Yu, T. Jiang, J. Li, Absorption spectroscopy gas sensor using a low-cost quartz crystal tuning fork with an ultrathin iron doped cobaltous oxide coating, Sens. Actuators B Chem. 326 (2021), 128951.

[31] Z. Lang, S. Qiao, Y. He, Y. Ma, Quartz tuning fork-based demodulation of an acoustic signal induced by photo-thermo-elastic energy conversion, Photoacoustics 22 (2021), 100272..

[32] C. Lou, X. Liu, Y. Wang, Y. Zhang, Y. Li, J. Yao, C. Chang, Y. Ma, X. Liu, Ultra-broadband optical detection from the visible to the terahertz range using a miniature quartz tuning fork, Opt. Lett. 47 (7) (2022) 1875–1878.

[33] Q. Zhang, J. Chang, Z. Cong, Z. Wang, Application of quartz tuning fork in photodetector based on photothermal effect, IEEE Photon. Technol. Lett. 31 (19) (2019) 1592–1595.

[34] U. Willer, A. Pohlkötter, W. Schade, J. Xu, T. Losco, R.P. Green, A. Tredicucci, H. E. Beere, D.A. Ritchie, Resonant tuning fork detector for THz radiation, Opt. Express 17 (16) (2009) 14069–14074.

[35] W. Ni, P. Lu, X. Fu, W. Zhang, P.P. Shum, H. Sun, C. Yang, D. Liu, J. Zhang, Ultrathin graphene diaphragm-based extrinsic Fabry-Perot interferometer for ultra-wideband fiber optic acoustic sensing, Opt. Express 26 (16) (2018) 20758–20767.

[36] C. Lin, Y. Liao, F. Fang, Trace gas detection system based on all-Optical quartz-enhanced photoacoustic spectroscopy, Appl. Spectrosc. 73 (11) (2019) 1327–1333.

[37] T. Lauwers, A. Glière, S. Basrour, An all-optical photoacoustic sensor for the detection of trace gas, Sensors 20 (2020) 3967.

[38] Q. Wang, Z. Wang, H. Zhang, S. Jiang, Y. Wang, W. Jin, W. Ren, Dual-comb photothermal spectroscopy, Nat. Commun. 13 (2022) 2181.

[39] F. Shen, A. Wang, Frequency-estimation-based signal-processing algorithm for white-light optical fiber Fabry-Perot interferometers, Appl. Opt. 44 (25) (2005) 5206–5214.

[40] K. Chen, Z. Yu, Z. Gong, Q. Yu, Lock-in white-light-interferometry-based all-optical photoacoustic spectrometer, Opt. Lett. 43 (20) (2018) 5038–5041.

[41] J. Xia, S. Xiong, F. Wang, H. Luo, Wavelength-switched phase interrogator for extrinsic Fabry-Perot interferometric sensors, Opt. Lett. 41 (13) (2016) 3082–3085.

[42] X. Qi, S. Wang, J. Jiang, K. Liu, P. Zhang, R. Li, T. Liu, Flywheel-like diaphragm-based fiber-optic Fabry–Perot frequency tailored acoustic sensor, J. Phys. D: Appl. Phys. 53 (2020), 415102.

[43] W. Zhang, P. Lu, Z. Qu, P. Fan, C. Sima, D. Liu, J. Zhang, High sensitivity and high stability dual Fabry-Perot interferometric fiber-optic acoustic sensor based on sandwich-structure composite diaphragm, IEEE Photon. J. 13 (2) (2021) 7100113.

[44] F.I.M. Ali, F. Awwad, Y.E. Greish, S.T. Mahmoud, Hydrogen sulfide (H_2S) gas sensor: a review, IEEE Sens. J. 19 (7) (2019) 2394–2407.

[45] M. Siciliani de Cumis, S. Viciani, S. Borri, P. Patimisco, A. Sampaolo, G. Scamarcio, P.D. Natale, F.D.' Amato, V. Spagnolo, Widely-tunable mid-infrared fiber-coupled quartz-enhanced photoacoustic sensor for environmental monitoring, Opt. Express 22 (23) (2014) 28222–28231.

[46] H. Wu, L. Dong, H. Zheng, X. Liu, X. Yin, W. Ma, L. Zhang, W. Yin, S. Jia, F.K. Tittel, Enhanced near-infrared QEPAS sensor for sub-ppm level H_2S detection by means of a fiber amplified 1582 nm DFB laser, Sens. Actuators B Chem. 221 (2015) 666–672.

[47] X. Tian, Y. Cao, J. Chen, K. Liu, G. Wang, X. Gao, Hydrogen sulphide detection using near-infrared diode laser and compact dense-pattern multipass cell, Chin. Phys. B 28 (6) (2019), 063301.

[48] K. Chen, B. Zhang, S. Liu, Q. Yu, Parts-per-billion-level detection of hydrogen sulfide based on near-infrared all-optical photoacoustic spectroscopy, Sens. Actuators B Chem. 283 (2019) 1–5.

[49] A. Varga, Z. Bozóki, M. Szakáll, G. Szabó, Photoacoustic system for on-line process monitoring of hydrogen sulfide (H_2S) concentration in natural gas streams, Appl. Phys. B 85 (2006) 315–321.

[50] X. Yin, L. Dong, H. Wu, W. Ma, L. Zhang, W. Yin, L. Xiao, S. Jia, F.K. Tittel, Ppb-level H_2S detection for SF_6 decomposition based on a fiber-amplified telecommunication diode laser and a background-gas-induced high-Q photoacoustic cell, Appl. Phys. Lett. 111 (2017), 031109.

[51] The HITRAN Database: ⟨http://www.hitran.com⟩.

[52] G.L. Long, J.D. Winefordner, Limit of detection: a closer look at the IUPAC definition, Anal. Chem. 55 (7) (1983) 712A–724A.

[53] R. Cui, L. Dong, H. Wu, W. Ma, L. Xiao, S. Jia, W. Chen, F.K. Tittel, Three-dimensional printed miniature fiber-coupled multipass cells with dense spot patterns for ppb-level methane detection using a near-IR diode laser, Anal. Chem. 92 (2020) 13034–13041.

[54] C. Lou, X. Yang, X. Li, H. Chen, C. Chang, X. Liu, Graphene-enhanced quartz tuning fork for laser-induced thermoelastic spectroscopy, IEEE Sens. J. 21 (8) (2021) 9819–9824.

[55] S.D. Russo, S. Zhou, A. Zifarelli, P. Patimisco, A. Sampaolo, M. Giglio, D. Iannuzzi, V. Spagnolo, Photoacoustic spectroscopy for gas sensing: a comparison between piezoelectric and interferometric readout in custom quartz tuning forks, Photoacoustics 17 (2020), 100155.

[56] J. Richling, Scratching the Surface - an Introduction to Photonics - Part 1 Optics, Thin Films, Lasers and Crystals, 2017.

Yufeng Pan is now pursuing a Ph.D. degree in optical engineering at Huazhong University of Science and Technology, China. He received his master's degree in atomic and molecular physics from Shanxi University, China, in 2021. His research interests include optical sensors and laser spectroscopy techniques.

Jinbiao Zhao is now pursuing a master degree in optical engineering in School of Optical and Electronic Information at Huazhong University of Science and Technology, China. His research interests include quartz-enhanced photoacoustic spectroscopy and trace gas detection.

Ping Lu is a Professor in School of Optical and Electronic Information at Huazhong University of Science and Technology, China, and Next Generation Internet Access National Engineering Laboratory. She got her Ph. D. degree on optical engineering in 2005 from Huazhong University of Science and Technology. Since 2006, she works at the School of Optical and Electronic Information at Huazhong University of Science and Technology, and starting from 2011, as full Professor. Her research mainly focused on fiber sensors, multicomponent trace gas detection, high sensitivity optical fiber acoustic detection technology and high resolution fiber sensor demodulation technology.

Chaotan Sima is an Associate Professor at Huazhong University of Science and Technology, China. He obtained the Ph.D. degree at the Optoelectronics Research Centre in the University of Southampton UK in 2013. He has been awarded the Marie-Curie Fellowship in 2019 and IEEE senior member since 2021. His research interests include advanced optical gas sensing, planar waveguide devices and holey optical fiber. He has been granted over 10 projects from National Natural Science Foundation of China and the National Key Research and Development Program of China etc. He serves as an editorial member of Optical and Quantum Electronics.

Wanjin Zhang is now pursuing a Ph.D. degree in optical engineering in School of Optical and Electronic Information at Huazhong University of Science and Technology, China. His research interests include optical sensors and high resolution fiber sensor demodulation technology.

Lujun Fu is now pursuing a Ph.D. degree in optical engineering in School of Optical and Electronic Information at Huazhong University of Science and Technology, China. His research interests include optical acoustic sensors and photoacoustic spectroscopy.

Deming Liu was born in Hubei Province, China, in January 1957. He received the Graduate degree from Chengdu Institute of Telecommunication (now University of Electronic Science and Technology of China), Chengdu, China, in 1984. Currently, he is the Professor of Huazhong University of Science and Technology, Wuhan, China. His recent research interests include optical access network, optical communication devices, and fiber-optic sensors.

Jiangshan Zhang is an Associate Professor in School of Electronic Information and Communications at Huazhong University of Science and Technology, China. He obtained the Ph.D. degree on information and communication Engineering in 2005 from Huazhong University of Science and Technology. His research interests include signal processing and digital communication.

Hongpeng Wu received his Ph.D. degree in atomic and molecular physics from Shanxi niversity, China, in 2017. From 2015–2016, he studied as a joint Ph.D. student in the Electrical and Computer Engineering Department and Rice Quantum Institute, Rice University, Houston, USA. Currently he is a professor in the Institute of Laser Spectroscopy of Shanxi University. His research interests include optical sensors and laser spectroscopy techniques.

Lei Dong received his Ph.D. degree in optics from Shanxi University, China, in 2007. From June, 2008 to December, 2011, he worked as a post-doctoral fellow in the Electrical and Computer Engineering Department and Rice Quantum Institute, Rice University, Houston, USA. Currently he is a professor in the Institute of Laser Spectroscopy of Shanxi University. His research activities research activities are focused on research and development in laser spectroscopy, in particular photoacoustic spectroscopy applied to sensitive, selective and real-time trace gas detection, and laser applications in environmental monitoring, chemical analysis, industrial process control, and medical diagnostics. He has published more than 100 peer reviewed papers with $>$ 2200 positive citations.